Effect of temperature on the current (capacitance and conductance)–voltage characteristics of Ti/*n*-GaAs diode

K. Ejderha,[1] S. Duman,[2,a)] C. Nuhoglu,[3] F. Urhan,[2] and A. Turut[4]
[1]*Department of Electricity and Energy, Vocational High School of Technical Sciences, Bingol University, 12000 Bingol, Turkey*
[2]*Department of Physics, Faculty of Sciences, Ataturk University, 25240 Erzurum, Turkey*
[3]*Department of Physics, Faculty of Sciences, Yildiz Technical University, 34220 Istanbul, Turkey*
[4]*Department of Engineering Physics, Faculty of Sciences, Istanbul Medeniyet University, 34700 Istanbul, Turkey*

(Received 19 September 2014; accepted 9 December 2014; published online 18 December 2014)

In this study, Ti/*n*-GaAs Schottky barrier diode has been fabricated by DC magnetron sputtering. The current–voltage, capacitance–voltage, and conductance–voltage characteristics of Ti/*n*–GaAs diode have been investigated in the temperature range of 80–320 K. The ideality factor and barrier height values have been calculated from the forward current–voltage characteristics. The variation of the diode parameters with the sample temperature has been attributed to the presence of the lateral inhomogeneities of the barrier height. The temperature dependent capacitance–voltage characteristics have been measured to calculate the carrier concentration, diffusion potential, barrier height, and temperature coefficient of the barrier height ($\alpha = -0.65\,\text{meV K}^{-1}$). The fact that the temperature coefficient of the barrier height changes from metal to metal has been ascribed to the chemical nature of the contact metal or metal electronegativity. © *2014 AIP Publishing LLC*. [http://dx.doi.org/10.1063/1.4904918]

I. INTRODUCTION

Schottky barrier diodes (SBDs) are among the most simple metal-semiconductor (MS) contact devices, and a full understanding of the nature of their electrical characteristics is of greater interest.[1] An MS contact is one of the most widely used rectifying contact type in the electronics industry.[2,3] The current–voltage (*I–V*) and capacitance–voltage (*C–V*) characteristics of Ti/*n*–GaAs Schottky diodes have been studied by several authors.[4–7]

GaAs is the most technologically important and the most studied compound semiconductor material. Schottky contacts on GaAs have been widely used in SBDs, metal-semiconductor field-effect transistors (MESFETs) for microwave communication and high-speed microelectronic applications, and other microwave communication devices.[1,5]

Some researchers have performed the temperature dependent *I–V* measurements of the Ti/*n*-GaAs diodes fabricated by different deposition techniques to determine both their Schottky barrier height (SBH) and ideality factor.[4–7] Among the deposition techniques, the sputtering is widely used because it has the advantage that the deposition rate and substrate temperature are easily controlled and metals with very high melting point can be deposited.[5] An advantageous feature is the good adherence of these contacts, which plays an important role in the preparation of clean surfaces. The bombardment of the substrate by electrons, ions, and neutral atoms from the sputtering gas generates defects into the semiconductor substrate and creates the same type of defects on Si, Ge, GaAs, and InP.[1,6,8] Nevertheless, as well as the possible defect formation during metal deposition, it has been reported that the plasma techniques such as r.f. or d.c. sputtering can lead to passivation of the interfacial defects during the sputter metallization process. Moreover, related techniques such as sputter etching and reactive ion etching play an important role in the preparation of clean surfaces. The presence of a passivated layer produces a deterioration of the metal-semiconductor interface properties and may have significant effects on the carrier transport through the barrier.[5–11]

In the present study, Ti/*n*-GaAs SBD has been prepared by DC magnetron sputtering deposition. The *I–V*, *C–V*, and conductance-voltage (*G–V*) characteristics of the Ti/*n*-GaAs diode have been measured in the temperature range of 80–320 K in steps of 20 K. The values of barrier height and temperature coefficient for diode have been compared with those obtained by several authors using different deposition processes. The *I–V* and *C–V* characteristics of the Ti/*n*-GaAs are already documented in the literature, but to the best of our knowledge, the temperature dependence of the *G–V* characteristics in Ti/*n*-GaAs SBDs fabricated by dc magnetron sputtering technique has not yet been studied in the literature.

II. EXPERIMENTAL PROCEDURE

The samples were prepared using cleaned and polished *n*-GaAs (as received from the manufacturer) with (100) orientation and $7.62 \times 10^{15}\,\text{cm}^{-3}$ carrier concentrations. Before making contacts, the *n*-GaAs wafer was dipped in $5H_2SO_4 + H_2O_2 + H_2O$ solution for 1 min to remove the surface damaged layer and undesirable impurities, then in a solution of $H_2O + HCl$. Preceding each cleaning step, the

a)Author to whom correspondence should be addressed. Electronic mail: sduman@atauni.edu.tr.

wafer was rinsed thoroughly in de-ionized water with resistivity of 18 MΩ cm. The wafer has been dried with high-purity nitrogen and inserted into the deposition chamber immediately after the etching process. Ohmic contact on the back surface of *n*-GaAs was formed by vapour deposition of high purity (99.999%). Indium (In) metal was evaporated at a low pressure about 10^{-5} Torr through a thermal evaporation system. The thickness of the In layer is about 1000 Å. After the In deposition, the sample was annealed at 385 °C for 3 min for the formation of ohmicity. After annealing, the circular Schottky contacts with a diameter of 1.0 mm were formed on the front side of the *n*-GaAs wafer by magnetron DC sputtering. Titanium (Ti) is commonly used as a gate metal in the fabrication of GaAs field-effect transistors since it has good adhesion, stable against inter-diffusion, and compound formation, and moreover, it has good electrical properties at elevated temperatures.[6]

The *I-V* characteristics of the diode have been measured in the temperature range of 80–320 K using a Leybold Heraeus closed-cycle helium cryostat and a Keithley 487 Picoammeter/Voltage source under dark conditions. The *C-V* and *G-V* measurements of the diode have been performed using "Hewlett Packard" 4192A LF impedance analyser in the temperature range from 80 to 320 K in steps of 20 K.

III. RESULTS AND DISCUSSION

The current through a uniform metal-semiconductor interface due to thermionic emission (TE) can be expressed as (for $V \geq 3kT/q$)[2]

$$I = I_0\left[\exp\left(\frac{qV}{nkT}\right) - 1\right], \tag{1}$$

where I_0 is the saturation current defined by

$$I_0 = AA^*T^2\exp\left(-\frac{q\Phi_{b0}}{kT}\right), \tag{2}$$

where V, A, A^*, T, k, q, Φ_{b0}, and n are the forward-bias voltage, the effective diode area, effective Richardson constant for *n*-type GaAs, temperature in Kelvin, Boltzmann constant (8.625×10^{-5} eV/K), electronic charge, the zero bias (SBH), and ideality factor, respectively.

From Eq. (1), n can be written as

$$n = \frac{q}{kT}\left(\frac{dV}{d(\ln I)}\right), \tag{3}$$

n is introduced to take the deviation of the experimental *I–V* results from the ideal thermionic model into account or to include the contributions of other current transport mechanisms. It should be $n = 1$ for an ideal contact. Fig. 1 shows the forward bias *I–V* characteristics of Ti/*n*-GaAs SBD in the temperature range of 80–320 K by steps of 20 K.

As can be seen from Fig. 1, the current decreases depending on the temperature and reduced voltage at low temperatures of <300 K, i.e., the current decreases with the decreasing temperature for the same voltage value. The value of the application voltage required to reach the same current value increases. Using Eqs. (2) and (3) for the Ti/*n*-GaAs SBD, the experimental values of BH (Φ_{b0}) and ideality factor (n) were determined from the current axis intercept and the slope of the linear region of the forward bias characteristics at each temperature.

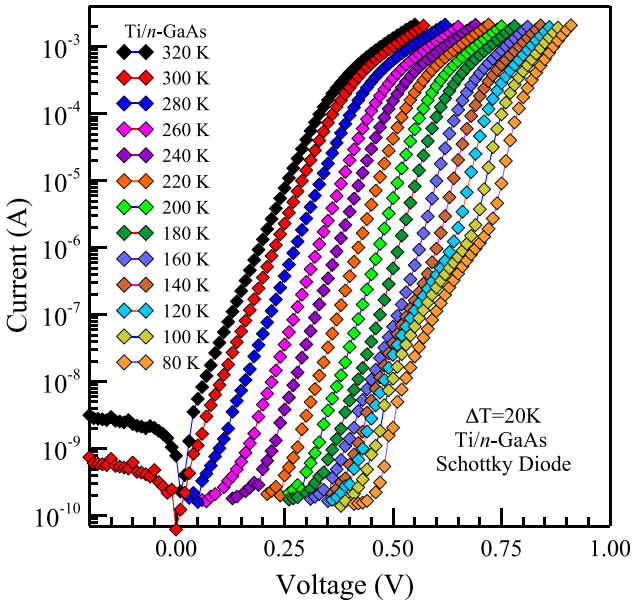

FIG. 1. The forward-bias current–voltage characteristics of Ti/*n*-GaAs SBD in the temperature range of 80–320 K.

Variation of the barrier height and ideality factor n with temperature has been given in Figs. 2 and 3. As can be seen from these figures, the BH increases and ideality factor decreases with the increasing temperature. These results are consistent with those of other studies given in the literature.[12,13] The barrier height is 0.80 eV for Ti/*n*-GaAs at 300 K. This value has been compared with that obtained by several authors using different deposition processes given in Table I. The calculated values of barrier height and ideality factor are consistent with most of these values.

A decrease in the experimental BH and an increase in the ideality factor n with a decrease in temperature may be attributed to the lateral inhomogeneities of the BHs in SBDs.[14] The inhomogeneities for Schottky barriers can be

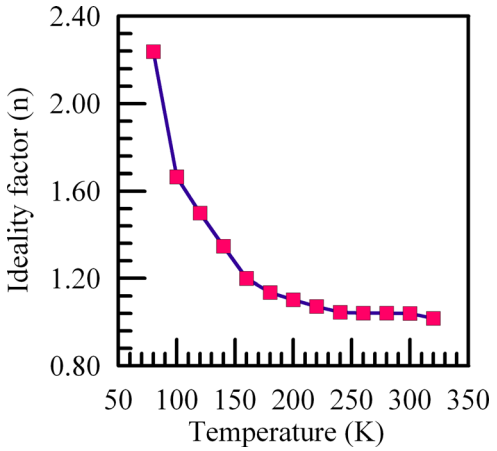

FIG. 2. Temperature dependence of the experimental ideality factor calculated from the *I–V* characteristics of Ti/*n*-GaAs diode.

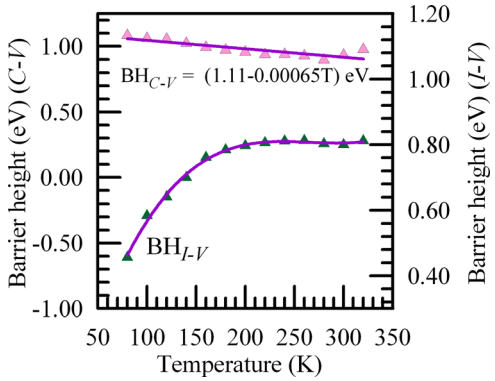

FIG. 3. Temperature dependence of the experimental barrier height calculated from the *I–V* and *C –V* measurements of Ti/n-GaAs diode.

attributed to different atomic phase, the effect of surface defects or interfaces, grain boundaries, and multiple phases.[1,12,14–16] One of them or more factors may dominate over the others in a certain temperature and voltage region. The experimental values of BH and n range from 0.46 eV and 2.24 at 80 K to 0.81 eV and 1.02 at 320 K, respectively. The ideality factor value of 1.04 for Ti/n-GaAs is very close to unity due to the homogeneity of the interface structure at 300 K. The barrier height is almost independent of the sample temperature in the temperature range of 180–320 K.

The potential fluctuations at the interface have low and high barrier areas. The current through the diode will flow preferentially through the lower barriers in the potential distribution at low temperatures. Since current transport across the MS interface is a temperature activated process at low temperatures, current will be dominated by current flowing through the patches with the lower SBH and larger ideality factor. As the temperature increases, the dominant BH will increase with the temperature and bias voltage, more electrons overcome the high potential barrier,[15–18] and so more current flows over the higher barrier regions. Therefore, the barrier height is high at higher temperatures, and most of the current flows through the low barrier regions at lower temperatures.[2,13,14] It is required to study in a wide temperature range to determine the parameters of MS contacts. The high values of n at low temperatures show that there is a deviation from the TE theory for the current mechanism. If the ideality factor is greater than 1 due to the thermionic field emission and recombination in depletion region, it must be temperature dependent.[3]

The $\ln(I_0/T^2)$ versus $(kT)^{-1}$ or $(nkT)^{-1}$ plots in Fig. 4 show the Richardson plots of the Ti/n-GaAs SBD according to Eq. (2). This $\ln(I_0/T^2)$ vs. $(kT)^{-1}$ plot shows significant

TABLE I. Ideality factor and barrier height values calculated from the lnI–V characteristics of Ti/n-GaAs diodes.

Diodes	Φ_b (eV)	n	Deposition technique	References
Ti/n-GaAs	0.80	1.04	DC magnetron sputtering	This work
Ti/n-GaAs	0.82	1.03	E-beam evaporation	4
Ti/n-GaAs	0.83 and 0.85	1.03–1.08	Ion beam sputtering	5
Ti/n-GaAs	0.90	1.02	DC magnetron sputtering	6
Ti/n-GaAs	0.698	1.05	Ion beam sputtering	7

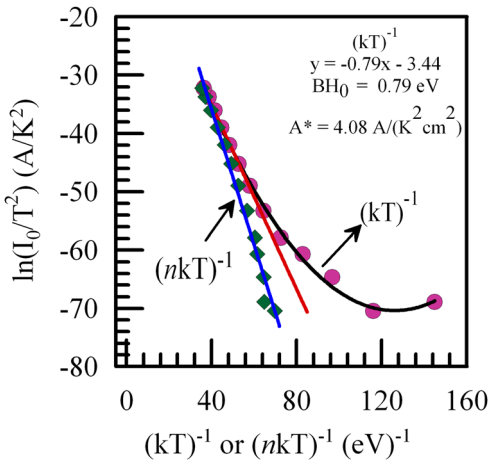

FIG. 4. The experimental plots $\ln(I_0/T^2)$ versus $(kT)^{-1}$ or $(nkT)^{-1}$ of Ti/n-GaAs diode.

deviation from linearity at low temperatures. The non-linearity of the conventional $\ln(I_0/T^2)$ versus $(kT)^{-1}$ is caused by the temperature dependence of the BH and n. The experimental results are seen to fit asymptotically to a straight line at higher temperatures only. The Richardson constant value of $A^* = 4.08$ A cm^{-2} K^{-2} is determined from the intercept at the ordinate of this experimental plot, which is much lower than the known value of 8.16 A cm^{-2} K^{-2} for n-GaAs and its slope gives the barrier height value as 0.79 eV. The deviation in the Richardson plots may be due to the presence of the spatially inhomogeneous BHs and potential fluctuations at the interface that consists of low and high barrier areas,[3,14–16,19–23] that is, when the temperature is lowered, the current through the diode will flow preferentially through the lower barriers in the potential distribution.[2,15,17] As indicated above, the conventional activation energy $\ln(I_o/T^2)$ vs. $(2kT)^{-1}$ plot has shown non-linearity at low temperatures. But $\ln(I_0/T^2)$ vs. $(nkT)^{-1}$ plot has yielded a straight line. Using the experimental I_0 data, a modified $\ln(I_0/T^2)$ vs. $(nkT)^{-1}$ plot gives a straight line with slope directly yielding the mean $\bar{\Phi}_{bo}$. From the straight-line, zero-bias mean BH was obtained $\bar{\Phi}_{bo} = 1.16$ eV in the range of 80–320 K.

As can be seen in Fig. 5, there is a linear correlation between the ideality factor and barrier height values and this

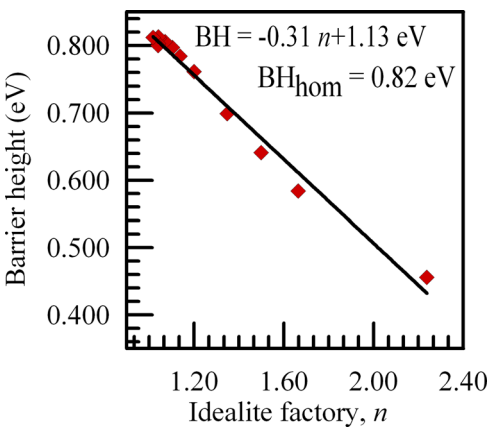

FIG. 5. Barrier height versus ideality factor plot for the Ti/n-GaAs SBD at various temperatures.

linear relationship can be explained by the lateral inhomogeneity of the barrier height.[12,24] In the 80–320 K temperature range, through the extrapolation of the Φ_{b0} versus n plot to $n=1$, homogenous BH values have been obtained as 0.82 eV in the case of $n=1$ in Fig. 5 for Ti/*n*-GaAs SBD.

The *C*–*V* measurements can give information about the formation of metal/semiconductor interface, device, and material characteristics and are widely used to determine the device parameters. The forward and reverse bias *C*–*V* measurements of the Ti/*n*–GaAs diode have been given in Fig. 6. The characteristics parameters of the Ti/*n*-GaAs rectifier diode such as barrier height, carrier concentration, diffusion potential, and the Fermi energy level can be calculated from the reverse bias C^{-2}–*V* characteristics in the temperature range of 80–320 K.[2,24] The C^{-2}–*V* characteristics of the diode from 1 to −1 V are shown in Fig. 7 and the capacitance value increases with the increasing temperature and the C^{-2}–*V* characteristic exhibits a linear variation.

As can be seen in Fig. 7, C^{-2}–*V* plots give a straight line in a wide range of applied bias voltages. The relation between capacitance and applied bias voltage for SBDs is expressed as[25–27]

$$C^{-2} = \frac{2(V_d + V)}{q\varepsilon_s\varepsilon_o A^2 N_d}, \tag{4}$$

where A is the area of diode, ε_s is the dielectric constant of the semiconductor (13.2 for n-GaAs),[2] N_d is the carrier concentration, q is the electron charge, V_d is the diffusion potential at zero bias, and V is applied voltage.

The derivative of Eq. (4) with respect to V is written as Eq. (5)

$$\frac{d(C^{-2})}{dV} = \frac{2}{q\varepsilon_s\varepsilon_o A^2 N_d}. \tag{5}$$

The value of V_d can be obtained from the intercept of C^{-2}–*V* plot by means of Eq. (4), and the N_d value can be obtained

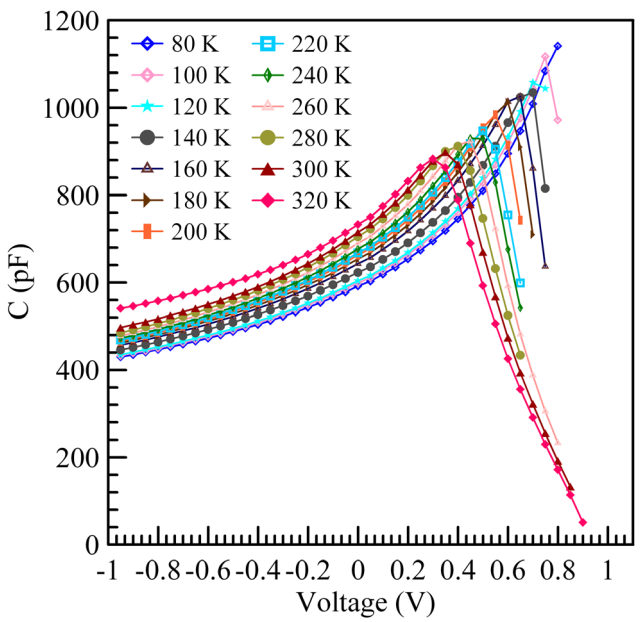

FIG. 6. The forward and reverse bias *C*–*V* characteristics of Ti/*n*-GaAs diode at various temperatures.

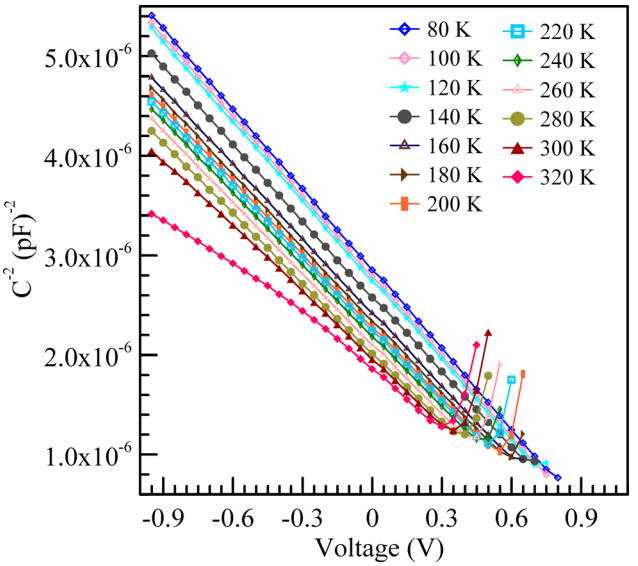

FIG. 7. The forward and reverse bias C^{-2}–*V* characteristics of Ti/*n*-GaAs diode at various temperatures.

from the slope of the C^{-2}–*V* plot by using Eq. (5), respectively.[2,28]

The BH Φ_b can be determined by using the following equation:

$$\Phi_b = V_d + V_n, \tag{6}$$

where V_n is the potential difference between the Fermi energy level and the top of the conduction band in the neutral region of diode. V_n can be calculated from the N_d and the density of states in the conduction band by the following equation:

$$V_n = kT\ln\left(\frac{N_d}{N_c}\right). \tag{7}$$

The effective density of states in the conduction band of GaAs equals $N_c = 4.71 \times 10^{17}\text{cm}^{-3}$.[24] It is found that these values determined from the C^{-2}–*V* curves depend on the measurement temperature. V_d, N_d, V_n, and Φ_b for the Ti/*n*-GaAs diode have the values of 1.07 V, 6.48 × 10^{16} cm^{-3}, 0.01 eV, and 1.08 eV at 80 K and 0.93 eV, 8.67 × 10^{16} cm^{-3}, 0.05 eV, and 0.98 eV at 320 K, respectively These values are given in Table II. The barrier height is 0.93 eV at 300 K and this value of barrier height is higher than that (0.80 eV) of *I*–*V* measurement.

The barrier height (BH) increased with a decrease in the temperature. Temperature dependence of the BH can be expressed with the following equation

$$\Phi_b(T) = \Phi_b(T=0) + \alpha T, \tag{8}$$

where $\Phi_b(T=0)$ is the BH extrapolated to T = 0 K, and α is the temperature coefficient of Φ_b $\Phi_{C\text{-}V} = 1.11(T=0) - 0.00065\,T$. Fig. 3 shows the variation of Φ_b as a function of temperature. The fitting of $\Phi_b(T)$ data in Eq. (8) yields $\Phi_b(T=0) = 1.11$ eV and this value is very close to the BH value of 1.16 eV from the modified Richardson plot $\ln(I_0/T^2)$ versus 1/(nkT) plot in Fig. 4. The Φ_b versus temperature plot

TABLE II. V_d, N_d, V_n, and Φ_b values calculated from the C^{-2}–V characteristics of Ti/n-GaAs diode.

Temperature (K)	V_d (V)	$N_d \times 10^{16}$ (cm^{-3})	V_n (eV)	Φ_b (eV)
80	1.07	6.48	0.01	1.08
100	1.04	6.49	0.02	1.06
120	1.03	6.53	0.02	1.05
140	1.00	6.75	0.02	1.02
160	0.97	6.95	0.03	1.00
180	0.94	7.01	0.03	0.97
200	0.92	7.06	0.03	0.95
220	0.90	7.18	0.04	0.94
240	0.90	7.19	0.04	0.94
260	0.89	7.30	0.04	0.93
280	0.85	7.35	0.05	0.90
300	0.89	7.83	0.05	0.94
320	0.93	8.67	0.05	0.98

from the reverse-bias C–V curves has given a BH temperature coefficient of $\alpha = -0.65$ meV/K. This value has been compared to the findings of other studies given in Table III. The temperature dependence of barrier height is due to the temperature dependence of the band gap.[17,29,30] This temperature coefficient value is close to the temperature coefficient value of the energy gap of GaAs (0.54 meV K^{-1}).[29,31,32] The fact that the BH temperature coefficient changes from metal to metal has been ascribed to the chemical nature of the contact metal or metal electronegativity. It has been stated that the temperature coefficient of the BH have been correlated to the chemical nature of the contact metal or metal electronegativity.[1,6]

The values obtained from I–V and C–V measurements for the barrier height are different. The values of the barrier height determined from the I–V measurements are lower than those obtained from the C–V measurements. This difference can be explained due to an interface layer or to trap states in the substrate, non-ideal interfaces, the effect of the image force and a spatial distribution of BHs due to barrier height inhomogeneities,[33–37] surface contamination at the interface, deep impurity levels, an intervening insulating layer, and quantum mechanical tunnelling.[13,16,25] The capacitance depends only on the mean band bending and is insensitive to the standard deviation of the barrier distribution.[14]

TABLE III. The temperature coefficient of the barrier height and band gap of n-GaAs.

	The temperature coefficient of the barrier height and band gap of n-GaAs (meV/K)	References
Ti/n-GaAs	−0.65	This work
n-type GaAs	−0.46	30
n- type GaAs	0.54	31
n- type GaAs	0.55	32
Au/n-GaAs	−0.23 ± 0.03	33
Au/n-GaAs	0.674	34
Cu/n-GaAs	−0.778	12
Cu/n-GaAs	−0.47 ± 0.02	39
Ti/n-GaAs	0.090	6

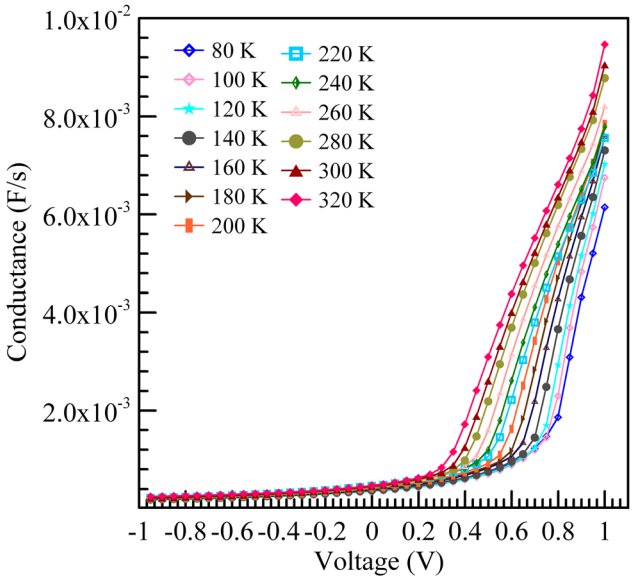

FIG. 8. The forward and reverse bias G–V characteristics of the Ti/n-GaAs diode at various temperatures.

The current in the I–V measurement is dominated by the current which flows through the region of low SBH. The measured I–V BH is significantly lower than the weighted arithmetic average of the SBHs. The C–V measured BH is influenced by the distribution of charge at the depletion region boundary and this charge distribution follows the weighted arithmetic average of the SBH inhomogeneity; hence, the BH determined by C–V is close to the weighted arithmetic average of the SBHs. Therefore, the SBH determined from the zero-bias intercept assuming thermionic emission as current transport mechanism is well below the C–V measured BH and the weighted arithmetic average of the SBHs.[14,17,38]

Fig. 8 depicts the G–V plots of the Ti/n-GaAs diode as a function of temperature in the range of 80–320 K and in the voltage range of −1.0–1.0 V. The measured conductance remained almost constant from −1.0 V to 0.0 V in the reverse bias. It has been seen that the value of conductance increases with the increasing temperature and applied voltage in the forward-bias.

IV. CONCLUSION

In this study, quality Ti/n-GaAs Schottky diode has been fabricated by using DC magnetron sputtering. The investigation of I–V, C–V, and G–V characteristics in the Ti/n-GaAs diode in the temperature range from 80 to 320 K has been reported. The values of ideality factor and barrier height extracted from I-V measurements are 1.04 and 0.80 eV at 300 K. The I–V measurements show that n is close to unity at room temperature, indicating that the main mechanism of the current flow through the diode is TE, as the temperature is decreased, n values increase and BH values decrease, and the Richardson plot deviates from linearity with the decreasing temperature. These variations have been attributed to the influence of the Schottky barrier inhomogeneities. In addition, significant deviation from linearity in the

Richardson plots with the decreasing temperature for the SBD has been observed. The *C-V* characteristics of the Ti/*n*-GaAs Schottky diode are also measured at different temperatures. The barrier height increased from 0.98 to 1.08 eV as the temperature decreased from 320 K to 80 K. A BH temperature coefficient value of $\alpha = -0.65$ meV/K has been obtained for this Ti/*n*-GaAs SBD, and this value is approximately equal to that of the energy gap in *n*-type GaAs.

[1]A. Turut, Turk. J. Phys. **36**, 235 (2012).
[2]E. H. Rhoderick and R. H. Williams, *Metal–Semiconductor Contacts* (Clarandon Press, Oxford University Press, 1988).
[3]D. Korucu and S. Duman, Thin Solid Films **531**, 436 (2013).
[4]K. Sinha, T. E. Smith, M. H. Read, and J. M. Poate, Solid-State Electron. **19**, 489 (1976).
[5]A. Cola, M. G. Lupo, L. Vasanelli, and A. Valentini, J. Appl. Phys. **71**, 4966 (1992).
[6]T. Goksu, N. Yildirim, H. Korkut, A. F. Ozdemir, A. Turut, and A. Kokce, Microelectron. Eng. **87**, 1781 (2010).
[7]Y. L. Jiang, G. P. Ru, F. Lu, X. P. Qu, B. Z. Li, W. Li, and A. Z. Li, Chin. Phys. Lett. **19**, 553 (2002).
[8]R. L. Van Meirhaeghe, L. M. O. Van Den Berghe, W. H. Laflere, and F. Cardon, Solid-State Electron. **31**, 1629 (1988).
[9]M. Di Dio, A. Cola, M. G. Lupo, and L. Vasanelli, Solid-State Electron. **38**, 1923 (1995).
[10]R. L. Van Meirhaeghe, W. H. Laflere, and F. Cardon, J. Appl. Phys. **76**, 403 (1994).
[11]K. Ejderha, A. Zengin, I. Orak, B. Tasyurek, T. Kilinc, and A. Turut, Mater. Sci. Semicond. Process. **14**, 5 (2011).
[12]M. Biber, Physica B **325**, 138 (2003).
[13]C. Coskun, S. Aydogan, and H. Efeoglu, Semicond. Sci. Technol. **19**, 242 (2004).
[14]J. H. Werner and H. H. Guttler, J. Appl. Phys. **69**, 1522 (1991).
[15]J. P. Sullivan, R. T. Tung, M. R. Pinto, and W. R. Graham, J. Appl. Phys. **70**, 7403 (1991).
[16]R. T. Tung, Phys. Rev. B **45**, 13509 (1992).
[17]A. F. Ozdemir, A. Turut, and A. Kokce, Semicond. Sci. Technol. **21**, 298 (2006).
[18]S. Dogan, S. Duman, B. Gurbulak, S. Tuzemen, and H. Morkoc, Physica E **41**, 646 (2009).
[19]Y. P. Song, R. L. Van Meirhaeghe, W. H. Laflere, and F. Cardon, Solid-State Electron. **29**, 633 (1986).
[20]E. Dobrocka and J. Osvald, Appl. Phys. Lett. **65**, 575 (1994).
[21]S. Zhu, R. L. Van Meirhaeghe, C. Detavernier, G. P. Ru, B. Z. Li, and F. Cardon, Solid State Commun. **112**, 611 (1999).
[22]S. Chand, Semicond. Sci. Technol. **17**, L36 (2002).
[23]R. E. Schmitsdorf, T. U. Kampen, and W. Mönch, Surf. Sci. **324**, 249 (1995).
[24]C. W. Wilmsen, *Physics and Chemistry of III-V Compound Semiconductor Interfaces* (Plenum Press, New York, 1995).
[25]S. M. Sze, *Physics of Semiconductor Devices* (Wiley, New York, 1981).
[26]S. Duman, B. Gurbulak, S. Dogan, and A. Turut, Vacuum **85**, 798 (2011).
[27]D. A. Neamen, *Semiconductor Physics and Devices* (Irwin, Boston, 1992).
[28]A. V. Ziel, *Solid State Physical Electronics*, 2nd ed. (Prentice-Hall, Englewood Cliffs, NJ, 1968).
[29]R. Passler, Phys. Rev. B **66**, 085201 (2002).
[30]I. Vurgaftman, J. R. Meyer, and L. R. Ram-Mohan, J. Appl. Phys. **89**, 5815 (2001).
[31]C. D. Thurmond, J. Electrochem. Soc. **122**, 1133 (1975).
[32]P. Lautenschlager, M. Garriga, S. Logothetidis, and M. Cardona, Phys. Rev. B: Condens. Matter **35**, 9174 (1987).
[33]M. Missous, E. H. Rhoderick, D. A. Woolf, and S. P. Wilkes, Semicond. Sci. Technol. **7**, 218 (1992).
[34]S. Karatas, Microelectron. Eng. **87**, 1935 (2010).
[35]M. Siad, A. Keffous, S. Mamma, Y. Belkacem, and H. Menari, Appl. Surf. Sci. **236**, 366 (2004).
[36]S. Forment, R. L. Van Meirhaeghe, A. De Vrieze, K. Strubbe, and W. P. Gomes, Semicond. Sci. Technol. **16**, 975 (2001).
[37]L. J. Brillson, Surf. Sci. Rep. **2**, 123 (1982).
[38]R. T. Tung, A. F. J. Levi, J. P. Sullivan, and F. Schrey, Phys. Rev. Lett. **66**, 72 (1991).
[39]S. Hardikar, M. K. Hudait, P. Modak, S. B. Krupanidhi, and N. Padha, Appl. Phys. A: Mater. Sci. Process. **68**, 49 (1999).